European Journal of Radiology Open 6 (2019) 106–112

Contents lists available at ScienceDirect

European Journal of Radiology Open

journal homepage: www.elsevier.com/locate/ejro

Digital subtract angiography and lipiodol deposits following embolization in cirrhotic nodules of LIRADS category ≥3

Zhen Kang*, Nan Wang, Anhui Xu, Liang Wang

Department of Radiology, Tongji Hospital, Tongji Medical College, Huazhong University of Science and Technology, No. 1095 Jiefang Road, Hubei, Wuhan, 430030, PR China

ARTICLE INFO

Keywords:
Liver imaging reporting and data system
Digital substract angiography
Lipiodol deposits

ABSTRACT

Purpose: To assess the correlation between Liver Imaging Reporting and Data System (LIRADS) and digital substract angiography (DSA) and lipiodol deposits in cirrhotic nodules of LIRADS category ≥3 receiving interventional treatment.

Methods: From June 2014 to June 2016, patients with cirrhotic nodules were identified retrospectively and MR images were reviewed by sub-specialty radiologists according to modified LIRADS v2014. Correlation between nodules of LIRADS category ≥3 and DSA findings and lipiodol deposits were analyzed.

Results: 71 cirrhotic nodules were evaluated in 33 patients. 39/71 nodules were classified as LR-3, 9/71 nodules were categorized as LR-4, 23/71 nodules were grouped into LR-5. 43 nodules presented positive DSA, 37 nodules showed presence of lipiodol deposits during follow up. With the upgrade of LIRADS category of cirrhotic nodules, DSA and lipiodol deposits became more conspicuous. Spearman analysis demonstrated positive correlations between LIRADS and DSA ($r = 0.567$, $P = 0.000$) as well as LIRADS and lipiodol deposits ($r = 0.616$, $P = 0.000$). ROC analysis revealed a cut-off value of LR ≥ 4 resulted in a sensitivity of 67.4% and specificity of 89.3% in predicting positive DSA (RUC = 0.799, $P < 0.0001$), and a sensitivity of 75.7% and specificity of 88.2% in predicting lipiodol deposits (RUC = 0.818, $P < 0.0001$). Of 39 lesions of LR-3, 64.1% (25/39) showed negative DSA, and 76.9% (30/39) showed absence of lipiodol deposits during follow up. Logistic regression analysis identified arterial enhancement (OR = 26.837, $P = 0.002$) and lesion size (OR = 1.325, $P = 0.022$) were independently associated with positive DSA in nodule of LIRADS category ≥3, while no factors were associated with lipiodol deposits.

Conclusion: The LIRADS can be used to predict DSA findings and lipiodol deposits in nodules with LIRADS score 3 and above. LIRADS 3 nodules tend to be DSA-negative and have less lipiodol deposits. DSA and lipiodol deposits become more conspicuous in nodules from LIRADS 3 to 5.

1. Introduction

Cirrhosis patients are prone to develop multiple nodules including regenerative nodules (RNs), dysplastic nodules (DNs) and hepatocellular carcinoma (HCC) [1]. 21% of indeterminate nodules discovered incidentally may progress toward HCC clinically or pathologically proven within 2 years [2]. For patients with multi-focal disease, resection showed inferiority to liver transplantation and transcatheter arterial (chemo) embolization (TACE or TAE) due to the cirrhosis background, concurrent multiple lesions and potential treatment-related complications such as liver failure [3]. According to the Barcelona Clinic Liver Cancer (BCLC) staging system for HCC, TACE serves as a palliative therapy for patients with large cancers or multifocal disease that are not amenable to curative treatments [4].

However, the imaging manifestations of these cirrhosis-related nodules in DSA and how they respond to interventional therapy have not been fully elaborated, and when to perform interventional therapy for these nodules have not been sufficiently studied and are subjects of considerable interest. On one hand, it might prevent the potential malignant transformation of these nodules during wait-list time or

Abbreviations: LIRADS, Liver Imaging Reporting and Data System; TACE, transcatheter arterial chemoembolization; TAE, transcatheter arterial embolization; DSA, digital subtract angiography; BCLC, Barcelona Clinic Liver Cancer; RN, regenerative nodules; DN, dysplastic nodules; HCC, hepatocellular carcinoma; RIS, radiology information system; PACS, picture archiving and communication system; T1WI, T1 weighted imaging; T2WI, T2 weighted imaging; PWI, perfusion weighted imaging; DWI, diffusion weighted imaging; LR-M, probably or definitely malignant but not specific for HCC

* Corresponding author.
E-mail address: kangzh15@hust.edu.cn (Z. Kang).

https://doi.org/10.1016/j.ejro.2019.02.005
Received 17 October 2018; Received in revised form 1 January 2019; Accepted 9 February 2019
Available online 23 February 2019

other therapies, but on the other hand, it may increase patients' financial burden because many nodules would remain stable within a long period of time [5]. Scrupulous analysis of these nodules is of great importance before undergoing TACE or TAE. Recent advances in MR imaging plays a vital role in detection and characterization of these nodules [6], and succedent Liver Imaging Reporting and Data System (LIRADS) could quantify the risk of developing HCC for patients with cirrhosis or other risk factors [7]. The LIRADS score helps indicate a relative risk for HCC with categorization from LR-1 to LR-5 in order (definitely benign, probably benign, intermediate, probably HCC and definitely HCC), among which cirrhosis-associated nodules LR ≥ 3 have a higher risk to develop into HCC comparing with lesions ≤ LR2.

In the present study, we aimed to characterize DSA findings and lipiodol deposits following transcatheter arterial (chemo)embolization in Cirrhotic Nodules of LIRADS Category ≥3.

2. Methods

2.1. Patients

This retrospective study was approved by our institutional review board, and written informed consent was waived. From June 2014 to June 2016 inclusively, the radiology information system (RIS) and picture archiving and communication system (PACS) database were retrospectively queried to identify all treatment-naïve patients with cirrhosis and multiple focal nodules on MRI. These nodules were subsequently reassessed by two sub-specialty radiologists using LIRADS v2014 and given a score, discrepancies were resolved by consensus. Flowchart for selection of the patient in the present study was shown in Fig. 1. Alpha-fetoprotein was elevated in 23/33 patients, normal in 6 patients and unavailable in 4 patients. These patients were subjected to DSA and therapeutic or prophylactic TA(C)E initially after a full discussion by our multidisciplinary treatment team in our hospital, which included hepatologists, oncologists, surgeons, and radiologists. Patients were informed about the details of the treatment procedure, including its possible benefits and risks of complications. The treatment choice was made at the patients' consent and therapy was arranged within 1 week, written informed consent was obtained from each patient.

2.2. MR scan protocol

MR examinations before TACE were performed in accordance with the established clinical standards of our institution using a 3.0 T magnet (GE Discovery MR 750, 32 channels Torso Upper coil). Each patient agreed to undergo examination after the purpose, methods, and risks were fully explained, and written informed consent was obtained from each patient. The protocols included T1 weighted imaging (T1WI), T2 weighted imaging (T2WI), perfusion weighted imaging (PWI), as well as diffusion weighted imaging (DWI) in some cases. Parameters for T2WI were: repetition time 10,000 ms, echo time 52.91 ms, slice thickness 6 mm, slice interval 7 mm, FOV 59.4 × 40 cm, NEX 2, EC 1. T1WI: repetition time 3.78 ms, echo time 1.71 ms, slice thickness 5 mm, slice interval 2.5 mm, FOV 56.4 × 38 cm, NEX 0.70, EC 1. DWI: repetition time 5000 ms, echo time 52 ms, slice thickness 6 mm, slice interval 7 mm, FOV 59.4 × 40 cm, NEX 1, EC 1, 12 b values from 50-1000. Parameters for PWI with fat saturation were identical with T1WI. The contrast used were Gd-DTPA (Bayer®) at the volume of 0.1 mmol/Kg and an injection rate of 2 ml/s.

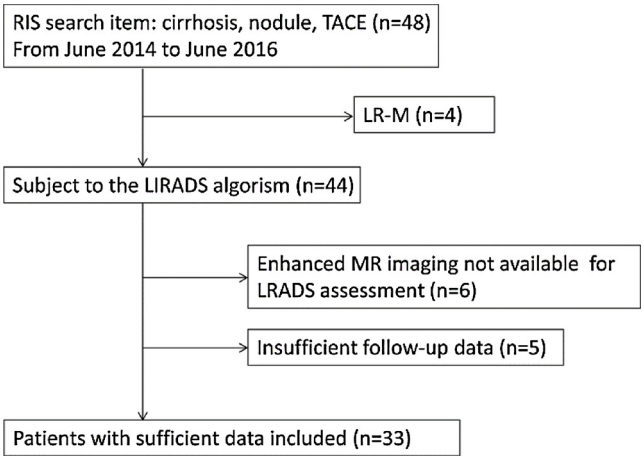

Fig. 1. Flowchart for selection of the patient in the present study.

Table 1
Modified LIRADS for category ≥3 nodules.

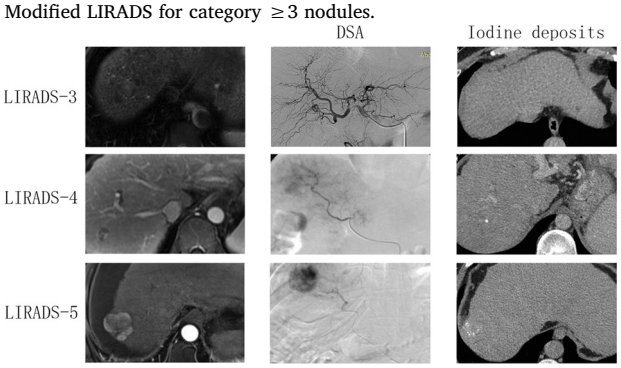

Observation in the "LR-4/LR-5″ is adjusted to LR-4 according to tie-breaking rules.

2.3. LIRADS scoring and imaging interpretation

LIRADS category of nodules was scored in accordance with the modified algorithm. Major imaging features include arterial phase enhancement, washout, and capsule appearance. Threshold growth of the hepatic observation were omitted because patients included in this study had all received the TACE procedure when diagnosed. The modified diagnostic algorithm was showed in Table 1. The reviewers were blinded to the clinical data of hepatic observations except for its location based on Couinaud's numbering system in order to guide the reviewers and facilitate precise evaluation. Only those determined not to be LR-M were assessed further on MRI. The presence of arterial enhancement, washout and capsule appearance were determined on MRI according to LIRADS v2014. If three or more nodules distributed in the liver, three "index lesions" with the largest diameter were analyzed. LR-4 was conservatively kept for the lesions with LR-4/5 according to the tie-breaking rules. One radiologist with 10-year experience on abdomen imaging interpretation reviewed the imaging first and the final LIRADS category modifications were verified by another radiologist with 15-year experience on abdomen imaging interpretation, discrepancies were resolved by consensus.

2.4. TACE procedure

Informed consent was obtained from all patients after the purpose and risks of the DSA and embolization procedure had been fully explained. The procedure was performed by an experienced radiologist who had 15 years of experience in TACE. After anesthesia of the right femoral artery sheath with 2% lidocaine and deposition of a 5 F arterial sheath, a 5 F vascular catheter was inserted into the celiac artery. Following conventional hepatic angiography, the vascular catheter was subsequently inserted super selectively into the branch of the hepatic artery feeding the lesion. If the conventional catheter could not go into the hepatic artery because of tortuousness, one 2.9 F microcatheter (Terumo, Japan) was used. The findings on DSA were recorded as positive or negative. Abnormal feeding vessels and contrast agent staining

was defined as positive, normal feeding vessels and absence of contrast agent staining was defined as negative. Chemoembolization was then performed when the lesions showed evidence of positive DSA findings. Ten milliliters of lipiodol mixed with 50 mg lobaplatin was slowly infused into the lesions and the maximum of the volume of chemotherapeutic agent is 20 ml. When the angiography was negative, only 3 ml superliquefied lipiodol was used for diagnostic and prophylactic embolization.

2.5. Follow-up and response

Follow-up data was collected by electronic medical record. CT or MRI with or without contrast enhanced examination 1 month to 11 months after the initial TACE treatment was obtained for evaluation of nodule response to TACE treatment. Nodule size changes and presence/absence of lipiodol deposits were recorded.

2.6. Statistical analysis

All categorical data are presented as percentages or absolute numbers, $\chi 2$ test was used for comparisons. Spearman rank correlation was used to analyze the correlation between LIRADS and DSA findings and lipiodol deposits. Receiver operating characteristic curves (ROC) was used to assess the predictive values of LIRADS in predicting DSA positivity and lipiodol deposits. For LR-3 lesions, univariate and multivariate analyses were performed to identify potential predictors of positive DSA and lipiodol deposits. Odds ratios (ORs) were calculated as an estimate of the risk associated with a particular variable, with 95% confidence intervals (CIs) based on binomial distributions. Statistical analyses were performed by using software (SPSS, version 19.0, Chicago, IL). $P < 0.05$ was considered to indicate a statistically significant difference.

3. Results

3.1. Clinical characteristics of the cohort

Forty-eight patients who fulfilled the diagnosis of cirrhosis and concurrent nodules were included initially, while four patients were classified as probably malignant not specific for HCC (LR-M), six patients had no enhanced MR imaging, 5 patients had insufficient follow-up data and thus were excluded. Thirty-three patients with seventy-one nodules were finally included. It consisted of 26 males and 7 females, with a mean age of 51.5 years. 12 patients were found to have only one apparent nodule in the liver, 2 nodules were found in 4 patients and more than 3 nodules were found in 17 patients in which 3 index lesions were analyzed. The demographic, clinical and nodule characteristics of patients are reported in Table 2.

3.2. Correlation between LIRADS category and DSA findings and lipiodol deposits

On the grounds of the modified diagnostic algorism and the major imaging features on MR, 39/71 nodules were classified as LR-3 (Fig. 2), 9/71 nodules were categorized as LR-4 (Fig. 3), and 23/71 nodules were grouped into LR-5 (Fig. 4). 43 nodules presented positive DSA findings, the other 28 nodules were DSA negative. LR-5 nodules had more DSA positivity than that of LR-4, and LR-4 nodules had more DSA positivity than that of LR-3. Spearman analysis showed a positive correlation between LIRADS category and DSA findings ($r = 0.567$, $P = 0.000$). A statistically significant difference was found in different LIRADS categories ($\chi 2 = 22.908$, $P = 0.000$). During the follow up, 7 nodules of LR-3 reduced in size, and the remaining 32 nodules were stable in size. Of LR-4 nodules, 4 decreased in size, 3 remained stable, 2 presented with enlargement. 8 out of 23 LR-5 nodules showed decrease in size during follow up, 11 remained stable while 4 showed increase in size. 37 nodules showed presence of lipiodol deposits, 9 in LR-3 nodules, 8 in LR-4 nodules, 20 in LR-5 nodules, the other 34 nodules were absent of lipiodol deposits. As for lipiodol deposits, there also existed a positive correlation ($r = 0.616$, $P = 0.000$) and a statistically significant difference within different LIRADS categories ($\chi 2 = 29.243$, $P = 0.000$) (Table 3), in which LR-5 nodules had more lipiodol deposit than that of LR-4 and LR-3 nodules.

3.3. ROC analysis: using LIRADS category to predict DSA findings and lipiodol deposits

ROC analysis were pooled to assess LIRADS category in predicting DSA positivity and lipiodol deposits, results showed with a cut-off value of LR ≥ 4, the sensitivity to predict DSA positivity was 67.4% and the specificity was 89.3% (RUC = 0.799 [95%CI 0.687-0.885], $P < 0.0001$) (Fig. 5). The sensitivity and specificity using LIRADS category ≥4 to predict lipiodol deposits was 75.7% and 88.2%, respectively (RUC = 0.818[95%CI 0.768-0.940], $P < 0.0001$) (Fig. 6).

3.4. Logistic regression analysis

Of the 39 lesions of LR-3, none presented washout on MR, 64.1% (25/39) showed negative DSA, and 76.9% (30/39) showed absence of lipiodol deposits. Logistic regression analysis was conducted to identify the risk factors of LR-3 lesions on MR associated with DSA positivity and lipiodol deposits. On univariate analysis at $P < 0.1$, arterial enhancement ($P = 0.006$), lesion size ($P = 0.028$) were associated with DSA positivity, washout and capsule appearance were not relevant factors. Capsule appearance ($P = 0.064$) was associated with lipiodol deposits, while arterial enhancement, lesion size and washout were not relevant. In multivariable logistic regression model, arterial enhancement (OR = 26.837, 95CI% (3.259–221.006), $P = 0.002$) and lesion size (OR = 1.325, 95CI% (1.041–1.687), $P = 0.022$) were independently associated with DSA positivity, while none of these factors were associated with lipiodol deposits.

4. Discussion

Pathologic studies of resected specimens from cirrhotic liver revealed associated small nodular lesions such as RN, DN, and DN with subfocus of HCC (early HCC) [1]. Characterization of small lesions in cirrhotic patients is extremely difficult due to the overlap of imaging features among different entities in the step-way of the hepatocarcinogenesis [8], making the treatment option controversial. On the stepwise from RN via DN to HCC, it would be easier to guide the treatment with a quantified diagnosis algorism. Liver Imaging Reporting and Data System (LIRADS) is induced to interpret and report imaging of the liver in patients at risk for hepatocellular carcinoma (HCC) [9] which could reduce variability in lesion interpretation by standardizing report structure and positively affect the care of at-risk patients [10,11]. Meanwhile, DSA can clarify the blood supply of nodules, which is helpful for diagnosis, and embolization when needed can prevent malignant transformation of nodules, provides an optimal choice for these patients who are not suitable to curative treatments due to the multifocal lesions and does not induce significant long-term worsening of liver function [12].

In this retrospective study, included patients received DSA and, if necessary, prophylactic embolization because of suspected malignant nodules of the liver or elevated alpha-fetoprotein. We tried to analyze DSA findings and lipiodol deposits following TA(C)E in cirrhotic nodules of LIRADS Category ≥3. DSA and lipiodol deposits can assist in nodule characterization and decision-making for treatment in the future. Some evidence showed that DSA is insensitive to small HCC (< or = 2 cm), carcinomatosis arising within nodules, and DN [13]. But in some cases, DSA and iodine CT do offer a considerable help if the nodules cannot be correctively diagnosed [13]. In our study, most of the

Table 2
Baseline and clinical data of 33 included patients.

Serial	Gender	Age(y)	Lesion number	Arterial phase enhancement	Diameter (mm)	Washout	Capsule	LR score	DSA	Follow-up examination	Follow-up time	size	Lipiodol deposit
1	F	64	2	hyper-, hypo-/iso-	11, 11	n, n	n, n	3, 3	n, n	CT	4months	→, →	n, n
2	M	56	2	hyper-	27, 22	n, y	n, y	4, 5	n, p	CT	2months	↓,↓	n, y
3	M	61	3	hypo-/iso-, hypo-/iso-, hypo-/iso-	11, 9, 8	n, n, n	n, n, n	3, 3, 3	n, n, n	CT, MRI	7months	→, →→	n, n, n
4	F	43	3	hyper-, hyper-, hyper-	11, 10, 9	n, n, n	n, n, n	3, 3, 3	n, n, n	CT, MRI	2months	→, →, →	n, n, n
5	M	73	3	hyper-, hyper-, hypo-/iso-	21, 31, 34	y, y, n	y, n, n	5, 5, 3	p, p, p	CT	3months	↑,→,→	n, y, n
6	M	29	1	hyper-	31	y	n	5	p	CT	3months	↓	y
7	M	46	1	hyper-	27	y	y	5	p	CT	1 month	→	y
8	M	43	3	hyper-	14, 14, 11	n, n, n	n, n, n	3, 3, 3	p, p, p	CT	2months	→, →, →	y, n, n
9	M	54	1	hyper-	40	y	y	5	p	CT	2months	→	y
10	M	38	3	hypo-/iso-	11, 14, 18	n, n, n	n, n, n	3	n, n, n	CT	2months	→, →, →	n, n, n
11	M	40	1	hyper-	8	y	n	4	n	MRI	1months	↑	y
12	M	52	3	hyper-	93, 36, 25	y, y, y	y, y, y	5, 5, 5	p, p, n	CT	1month	↑, ↑, ↑	y, n, n
13	F	53	3	hyper-, hyper-, hypo-/iso-	7, 7, 7	n, n, n	n, n, n	3, 3, 3	n, p, n	CT	2months	→, →, →	n, y, n
14	F	58	3	hyper-, hyper-, hyper-	7, 16, 37	y, y, y	y, y, y	4, 5, 5	p, p, p	CT	2months	→, →, →	y, y, y
15	M	58	1	hypo-/iso-	16	n	n	3	n	CT	2months	→	n
16	M	71	3	hyper-, hyper-, hyper-	21, 16, 10	y, y, n	y, y, n	5, 5, 4	p, p, p	CT	2months	→, →, →	y, y, y
17	F	42	1	hyper-	83	y	y	5	p	CT	2months	↓	y
18	M	63	3	hyper-, hypo-/iso-, hypo-/iso-	30, 12, 13	y, n, n	y, y, n	5, 3, 3	p, p, p	CT, MRI	1month	↓, ↓, ↓	y, y, n
19	M	75	3	hyper-	13, 10, 8	n, n, n	n, n, n	3, 3, 3	p, p, p	CT	2months	↓, ↓, ↓	y, y, n
20	M	57	1	hypo-/iso-	16	n	n	3	n	CT	1 month	→	n
21	M	41	2	hypo-/iso-	10, 8	n, n	n, n	3, 3	n, n	CT	2months	→, →	n, n
22	M	50	1	hypo-/iso-	9	y	y	4	p	CT	2months	↓	y
23	M	37	3	hyper-	47, 11, 9	y, y, y	y, y, y	5, 5, 4	p, p, p	CT	2months	↓,↓,↓	y, y, y
24	M	50	3	hypo-/iso-	10, 10, 9	n, n, n	n, n, n	3, 3, 3	n, n, n	CT, MRI	11months	→, →,→	n, n, n
25	M	69	3	hyper-, hypo-/iso-, hypo-/iso-	42, 27, 12	n, n, n	n, n, n	5, 3, 3	p, p, p	CT	2months	↓, ↓,↓	y, y, y
26	M	59	1	hyper-	70	y	n	5	p	CT	1month	→	y
27	M	45	3	hyper-	33, 15, 15	y, y, n	n, y, n	5, 4, 3	p, p, p	CT	10months	↓,↑,→	y, y, n
28	M	38	3	hypo-/iso-	18, 11, 11	n, n, n	n, n, n	3, 3, 3	n, n, n	CT	1months	→, →, →	n, n, n
29	F	43	2	hypo-/iso-	8,5	n, n	n, n	3, 3	n, n	CT	2months	→, →	y, n
30	M	44	1	hyper-	14	y	n	4	p	CT	1month	↓	y
31	F	63	1	hyper-	15	n	n	3	p	CT, MRI	2months	→	y
32	M	44	1	hyper-	26	n	y	5	p	CT	2months	→	y
33	M	41	3	hyper-	83, 22, 16	y, y, y	n, n, n	5, 5, 4	p, p, p	CT	1 month	→, →, →	y, y, y

M: Male; F: Female; y: yes; n: no; p: positive, n (column DSA): negative; ↑: size increase; ↓: size decrease; →: size remain stable.

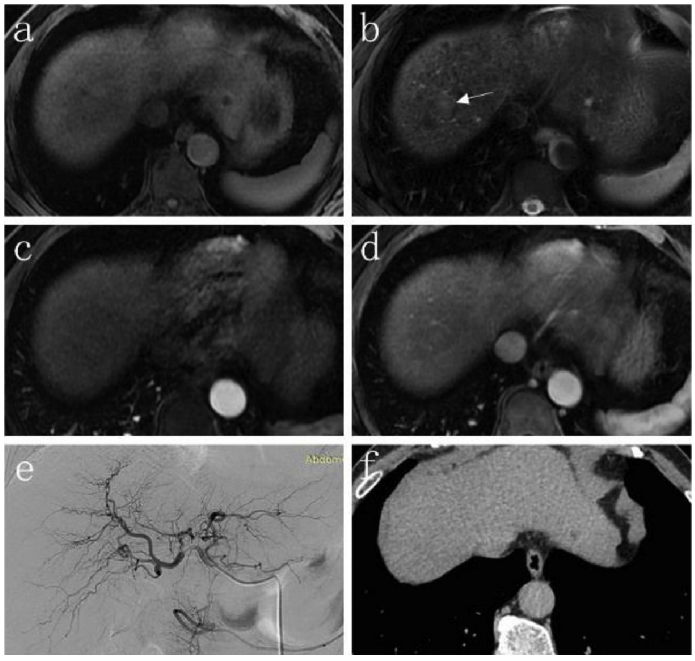

Fig. 2. LR-3 nodule and TAE outcome. An obscure nodule in segment 8 showed iso intensity on T1WI (A)and mild hyper intensity on T2WI (B), T1-weighted post-contrast demonstrated iso-enhancing relative to liver (C, D). This nodule was categorized in LR-3. DSA findings was negative (E), diagnostic and prophylactic embolization was merely performed. CT 6 weeks later showed absence of lipiodoldeposits (F).

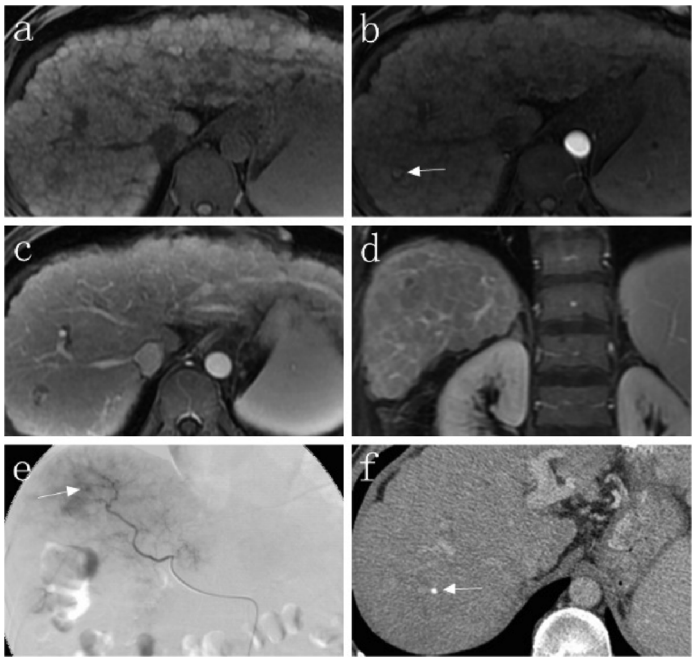

Fig. 3. LR-4 nodule and TACE outcome. An "index nodule" between segment 5 and 8 was noted in a cirrhosis patient, which showed T1 hypointense (A). Arterial phase of enhancement showed centric foci of enhancement (B). The nodule washed out on portal venous phase (C). This nodule was grouped into LR-4. DSA showed abnormality of hepatic arteries (E), which favors a diagnosis of HCC. 11 months later, CT showed a "dot" high intensity which was lipiodol in the lesion (F).

LR-3 nodules were in hypo vascularity with 64.1% (25/39) showed DSA negativity, the corresponding data for LR-4 and LR-5 nodules were 77.8% and 95.6%, respectively. It is noted that the higher LIRADS scoring, the more conspicuous these nodules will exhibit positivity on DSA. The pathway from an indeterminate nodule to HCC involves capillarization and neoangiogenesis, leading to a gradual change in blood supply from portal to arterial. These changes in intranodular blood supply create different enhancement pattern [14], which could be detected both in enhanced MR and DSA. A positive correlation between LIRADS category and DSA findings was found in our study, indicating an increased vascularity with the upward of LIRADS category and the necessity of DSA and following TA(C)E.

The amount of intratumoral lipiodol deposition was demonstrated to be associated with tumor necrosis, tumor residual, tumor recurrence and survival rate after TA(C)E. Accurate assessment of lipiodol

Table 3
Correlation between LIRADS category and DSA findings and Lipiodoldeposit.

LIRADS	DSA		Lipiodoldeposit	
	+	–	+	–
3	14	25	9	30
4	7	2	8	1
5	22	1	20	3
r	r = 0.567, p = 0.000		r = 0.616, p = 0.000	
$\chi 2$	$\chi 2$ = 22.908, p = 0.000		$\chi 2$ = 29.243, p = 0.000	

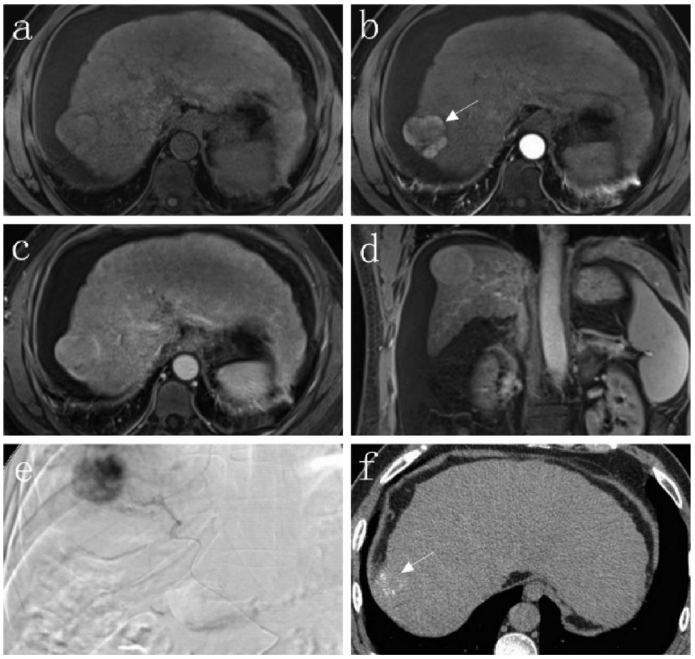

Fig. 4. LR-5 nodule and TACE outcome. T1-weighted (A) and T1-weighted post-contrast arterial phase (B, C, D) MRI showed a nodular external contour of the liver in segment 7 with hypervascularity on DSA (E), representing hepatocellular carcinoma. 2 months later, dispersed lipiodoldeposits were noted (F).

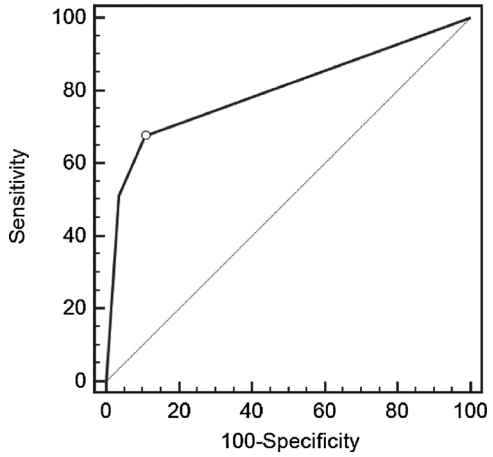

Fig. 5. Using LIRADS category to predict DSA findings. With a cut-off of LR ≥ 4, the sensitivity to predict DSA positivity was 67.4% and the specificity was 89.3%, RUC = 0.799 [95%CI 0.687-0.885], P < 0.0001.

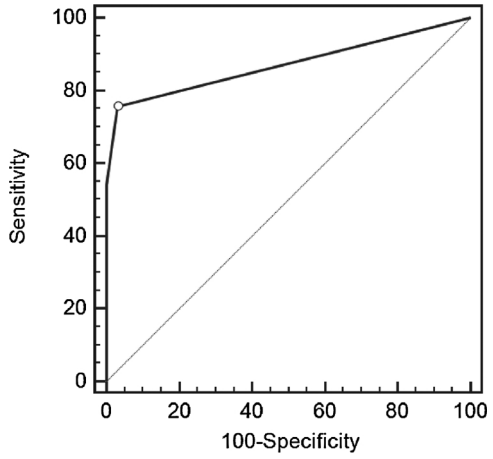

Fig. 6. Using LIRADS category to predict lipiodoldeposits. The threshold of LR ≥ 4 resulted in a 75.7% sensitivity and a 88.2% specificity in predicting lipiodoldeposits, RUC = 0.818[95%CI 0.768-0.940], P < 0.0001.

deposition is essential for liver tumor after TA(C)E and provides interventional radiologist with better information to evaluate the outcome of interventional therapy [15]. In our study, only 23.1% (9/39) of LR-3 nodules showed presence of lipiodol deposits, while 88.9% of LR-4 nodules and 87% of LR-5 nodules had lipiodol deposits. During follow up, 82% of LR-3 nodules were stable in size, this is in consistency with previous study [5]. While in LR-4 and LR-5 nodules, the corresponding percentages were 33.3% and 47.8%. The more lipiodol deposits, the more likely it is to indicate a tumor, and the more closely it is necessary to observe the change of tumor size during follow-up.

DSA findings and lipiodol deposits are also of usefulness to guide the next treatment [16]. Our study demonstrated a good positive correlation between LIRADS category and positive DSA findings and lipiodol deposits. A further ROC analysis showed both DSA and lipiodol deposits can be predicted by LIRADS category, in which the highest sensitivity and specificity could be achieved with a cut-off value of LR ≥ 4.

Whether LR-3 nodules should be subjected to DSA and interventional therapy when needed is clinically controversial, we further intensively analyzed the risk factors relating to DSA positivity among the LR-3 nodules. Our results showed that arterial enhancement and lesion size were independently associated with DSA positivity. And that indeterminate nodules with arterial enhancement were more likely to develop into HCC [2], indicating prophylactic embolization might be considered. However, none of arterial enhancement, nodule size, washout and capsule appearance was found to be associated with lipiodol deposits based on multivariable analysis. The inconformity may be attributable to the intranodular angiodysplasia which could not yet retain lipiodol. But on univariate analysis in our study, capsule appearance was proved to be associated with lipiodol deposits, meanwhile, newly visualized capsule was proved to be a predictor of upgrade and a higher possibility to progress although this feature is uncommon in LR-3 nodules [17,18]. Altogether, DSA and embolization treatment might be retained for selected patients with LR-3 nodules, and radiologists should closely surveil these nodules with arterial enhancement, large size and capsule appearance.

This study compared nodules of different LIRADS categories and their DSA findings and lipiodol deposit following requisite or prophylactic embolization, and we have proved a correlation between them. We chose MR LIRADS to analyze on account of that MR has a better performance comparing with CT [19] in characterizing the LIRADS algorism, because a substantial discordance about 77.2% between CT and MR exist in LIRADS category observations [20]. However, there are several limitations in our study. This study is in retrospective design, a relatively small sample size may limit the reliability, and applicability of the evaluation. In addition, 3 index lesions were selected for analysis if there were multiple cirrhosis-related nodules distributed in a patient's liver. Finally, short follow-up time is also a deficiency. Thus, a further prospective study with larger sample and long-term follow-up is recommended, to explore the prognosis of upgrade or downgrade of these nodules following interventional treatment.

5. Conclusion

In conclusion, we confirm that LIRADS score is correlated with DSA findings and lipiodol deposits, and it can be used to predict DSA findings and lipiodol deposits in nodules with LIRADS score 3 and above. Nodules with low LIRADS score tend to be DSA-negative and less lipiodol deposition. DSA and lipiodol deposits become more conspicuous in nodules from LIRADS 3 to 5.

Funding

This study was supported by grants from the National Natural Science Foundation of China (NSFC), Nos. 81171307 and 81671656.

Declaration of interest

The authors do not have any conflict of interest to declare.

References

[1] B.I. Choi, Hepatocarcinogenesis in liver cirrhosis: imaging diagnosis, J. Korean Med. Sci. 13 (1998) 103–116, https://doi.org/10.3346/jkms.1998.13.2.103.
[2] E.W. Beal, S. Albert, M. McNally, L.A. Shirley, J. Hanje, A.J. Michaels, et al., An indeterminate nodule in the cirrhotic liver discovered by surveillance imaging is a prelude to malignancy, J. Surg. Oncol. 110 (2014) 967–969, https://doi.org/10.1002/jso.23765.
[3] A. Forner, J.M. Llovet, J. Bruix, Hepatocellular carcinoma, Lancet 379 (2012) 1245–1255, https://doi.org/10.1016/S0140-6736(11)61347-0.
[4] J. Bruix, M. Sherman, Management of hepatocellular carcinoma, Hepatology (Baltimore, Md.) 42 (2005) 1208–1236, https://doi.org/10.1002/hep.20933.
[5] J.Y. Choi, H.C. Cho, M. Sun, H.C. Kim, C.B. Sirlin, Indeterminate observations (liver imaging reporting and data system category 3) on MRI in the cirrhotic liver: fate and clinical implications, AJR Am. J. Roentgenol. 201 (2013) 993–1001, https://doi.org/10.2214/AJR.12.10007.
[6] G.C. Mueller, H.K. Hussain, R.C. Carlos, H.V. Nghiem, I.R. Francis, Effectiveness of MR imaging in characterizing small hepatic lesions: routine versus expert interpretation, AJR Am. J. Roentgenol. 180 (2003) 673–680, https://doi.org/10.2214/ajr.180.3.1800673.
[7] D.G. Mitchell, J. Bruix, M. Sherman, C.B. Sirlin, LI-RADS (Liver Imaging Reporting and Data System): summary, discussion, and consensus of the LI-RADS Management Working Group and future directions, Hepatology (Baltimore, Md.) 61 (2015) 1056–1065, https://doi.org/10.1002/hep.27304.
[8] M. Di Martino, M. Anzidei, F. Zaccagna, L. Saba, S. Bosco, M. Rossi, et al., Qualitative analysis of small (< /=2 cm) regenerative nodules, dysplastic nodules

and well-differentiated HCCs with gadoxetic acid MRI, BMC Med. Imaging 16 (2016) 62, https://doi.org/10.1186/s12880-016-0165-5.
[9] C. An, G. Rakhmonova, J.Y. Choi, M.J. Kim, Liver imaging reporting and data system (LI-RADS) version 2014: understanding and application of the diagnostic algorithm, Clin. Mol. Hepatol. 22 (2016) 296–307, https://doi.org/10.3350/cmh.2016.0028.
[10] A.S. Purysko, E.M. Remer, C.P. Coppa, H.M. Leao Filho, C.R. Thupili, J.C. Veniero, LI-RADS: a case-based review of the new categorization of liver findings in patients with end-stage liver disease, Radiographics 32 (2012) 1977–1995, https://doi.org/10.1148/rg.327125026.
[11] A. Shah, A. Tang, C. Santillan, C. Sirlin, Cirrhotic liver: what's that nodule? The LI-RADS approach, J. Magn. Reson. Imaging 43 (2016) 281–294, https://doi.org/10.1002/jmri.24937.
[12] E. Caturelli, D.A. Siena, S. Fusilli, M.R. Villani, G. Schiavone, M. Nardella, et al., Transcatheter arterial chemoembolization for hepatocellular carcinoma in patients with cirrhosis: evaluation of damage to nontumorous liver tissue-long-term prospective study, Radiology 215 (2000) 123–128, https://doi.org/10.1148/radiology.215.1.r00ap21123.
[13] G.A. Krinsky, M.T. Nguyen, V.S. Lee, R.J. Rosen, A. Goldenberg, N.D. Theise, et al., Dysplastic nodules and hepatocellular carcinoma: sensitivity of digital subtraction hepatic arteriography with whole liver explant correlation, J. Comput. Assist. Tomogr. 24 (2000) 628–634 DN. PMID: 10966200.
[14] S.C. Efremidis, P. Hytiroglou, The multistep process of hepatocarcinogenesis in cirrhosis with imaging correlation, Eur. Radiol. 12 (2002) 753–764, https://doi.org/10.1007/s00330-001-1142-z.
[15] W.L. Monsky, I. Kim, S. Loh, C.S. Li, T.A. Greasby, L.S. Deutsch, et al., Semiautomated segmentation for volumetric analysis of intratumoral ethiodol uptake and subsequent tumor necrosis after chemoembolization, AJR Am. J. Roentgenol. 195 (2010) 1220–1230, https://doi.org/10.2214/AJR.09.3964.
[16] Y. Minami, M. Kudo, T. Kawasaki, M. Kitano, H. Chung, K. Maekawa, et al., Transcatheter arterial chemoembolization of hepatocellular carcinoma: usefulness of coded phase-inversion harmonic sonography, AJR Am. J. Roentgenol. 180 (2003) 703–708, https://doi.org/10.2214/ajr.180.3.1800703.
[17] M. Tanabe, A. Kanki, T. Wolfson, E.A. Costa, A. Mamidipalli, M.P. Ferreira, et al., Imaging outcomes of liver imaging reporting and data system version 2014 category 2, 3, and 4 observations detected at CT and MR imaging, Radiology 281 (2016) 129–139, https://doi.org/10.1148/radiol.2016152173.
[18] L.M. Burke, K. Sofue, M. Alagiyawanna, V. Nilmini, A.J. Muir, K.R. Choudhury, et al., Natural history of liver imaging reporting and data system category 4 nodules in MRI, Abdom. Radiol. (NY) 41 (2016) 1758–1766, https://doi.org/10.1007/s00261-016-0762-3.
[19] Y.D. Zhang, F.P. Zhu, X. Xu, Q. Wang, C.J. Wu, X.S. Liu, et al., Liver imaging reporting and data system: substantial discordance between CT and MR for imaging classification of hepatic nodules, Acad. Radiol. 23 (2016) 344–352, https://doi.org/10.1016/j.acra.2015.11.002.
[20] M.T. Corwin, G. Fananapazir, M. Jin, R. Lamba, M.R. Bashir, Differences in liver imaging and reporting data system categorization between MRI and CT, AJR Am. J. Roentgenol. 206 (2016) 307–312.